

# Mechanical properties of hemp fibre reinforced cement: Influence of the fibre/matrix interaction

D. Sedan<sup>a,\*</sup>, C. Pagnoux<sup>b</sup>, A. Smith<sup>a,\*</sup>, T. Chotard<sup>a,c,\*\*</sup>

<sup>a</sup> *Groupe d'Etude des Matériaux Hétérogènes (GEMH, EA 3178), Ecole Nationale Supérieure de Céramique Industrielle, 47 à 73 Avenue Albert Thomas, 87065 Limoges Cedex, France*

<sup>b</sup> *Laboratoire de Science des Procédés Céramiques et Traitements de Surface (SPCTS, UMR 6638 CNRS), Ecole Nationale Supérieure de Céramique Industrielle, 47 à 73 Avenue Albert Thomas, 87065 Limoges Cedex, France*

<sup>c</sup> *Institut Universitaire de Technologie, Département Génie Mécanique et Productique, 2 allée André Maurois, 87065 Limoges Cedex, France*

Received 1 March 2007; accepted 28 May 2007

Available online 6 August 2007

## Abstract

In this paper, preliminary results about both the chemical and physical behaviours of hemp fibres in calcium rich medium are presented. The influence of hemp fibres introduction in Portland cement pastes on the setting time has been investigated. It seems that pectin contained in the fibres can form complex molecules with calcium ions and could be responsible for the observed delay. The role of fibres surface treatment has been also studied. Chemical attack of the fibres surface by an alkaline and calcium rich solution degrades hemicelluloses contained in the fibres and seems to roughen the surface. This surface modification seems to play a major role in the strengthening of the cement/fibres interface. These results show that hemp fibres introduced in cement pastes exhibit a typical composite behaviour compared to cement sample, which lead to an improvement of the mechanical properties.

© 2007 Elsevier Ltd. All rights reserved.

**Keywords:** Cement; Composite; Mechanical properties

## 1. Introduction

In recent years, there has been a growing interest for the use of natural fibres in composite applications, where cellulose fibres act mostly as reinforcer of polymeric matrix.<sup>1</sup>

As a result of the increasing demand for environmentally friendly materials and the high cost of synthetic fibres such as carbon, glass or aramid, new bio-based materials containing natural fibres were developed. They are low density materials yielding relatively lightweight composites, which can exhibit high tensile strength and Young's modulus, as shown in previous studies for hemp, ramie, jute, sisal or softwood kraft.<sup>1</sup> These

fibres are renewable and cheap compared to processed fibres. Recent advances in the use of natural fibres (e.g., flax, cellulose, jute, hemp, kenaf, sisal, coir and bamboo) in composites have been reviewed by several authors.<sup>2–5</sup> Conventional fibres, like glass and carbon fibres, can be produced with a definite range of reproducible characteristics, whereas the properties of natural fibres vary considerably depending on the fibre diameter, structure (e.g. type of cellulose, nature of defects, orientation of the chains of non-crystalline cellulose and crystalline fibrils, proportion of crystalline fibrils and non-crystalline regions, spiral angle), supramolecular structure (degree of crystallinity), degree of polymerisation, void structure (pore volume, specific interface, size of pores) and whether the fibres come from the plant stem, leaf or seed.<sup>6</sup> Climatic conditions, age and the digestion process influence on the chemical composition of the fibres and their chemical characteristics. Depending on their origin, natural fibres can be grouped into hair, bast or hard fibres. Bast (flax, hemp, jute) and hard fibres (sisal, coir) are commonly used in composites.<sup>7</sup>

\* Corresponding authors.

\*\* Corresponding author at: Groupe d'Etude des Matériaux Hétérogènes (GEMH, EA 3178), Ecole Nationale Supérieure de Céramique Industrielle, 47 à 73 Avenue Albert Thomas, 87065 Limoges Cedex, France.

E-mail addresses: [d.sedan@ensci.fr](mailto:d.sedan@ensci.fr) (D. Sedan), [a.smith@ensci.fr](mailto:a.smith@ensci.fr) (A. Smith), [t.chotard@ensci.fr](mailto:t.chotard@ensci.fr) (T. Chotard).

Table 1  
Chemical analysis of hemp (wt.%)

	Cellulosic residue	Pectins	Hemicelluloses	Lignins	Others (waxes, fats, proteins, ashes)
Hemp fibres	56.1	20.1	10.9	6	7.9

In the building industry, one major challenge is the reduction of the carbon dioxide production during the manufacture of cement. There are two sources of carbon dioxide: decarbonation of limestone and combustion of fuel.<sup>8</sup> In such a context, there is a need to develop concrete with less cement but still a good durability. One possibility is to use natural fibres. Hemp is one example and it has been used for a long time in traditional constructions. The available literature data on these “eco-friendly” cement based composites containing natural fibres concern mainly their mechanical behaviour.<sup>9–11</sup> However, improvement of the mechanical characteristics implies good quality interfaces between the inorganic matrix and the fibres. So, before manufacturing such “eco-friendly” composites, it is necessary to understand the nature of surface interactions between the matrix and the fibres. For instance, it is reported that natural fibres introduced in a cement paste delay the setting time<sup>12</sup> without any real explanation to this phenomenon. So, it seems interesting to identify factors responsible for this delay in setting time in order to have a good understanding of interactions between fibres and cement, and to examine how to modify the fibre surface by an appropriate treatment in order to increase physical and mechanical properties of such “eco-friendly” composites.

The aim of this research is to examine the behaviour of hemp fibres in a cement matrix. So, after having described the materials and the methods, we will study the chemical interactions between the matrix and its reinforcement to finally explain the mechanical behaviour of such composite.

## 2. Materials and methods

### 2.1. Materials

#### 2.1.1. Raw materials

Cortical hemp fibres used in this work were supplied by la Chanvrière de l’Aube (Bar-sur-Aube, France). Their density, measured with a pycnometer (Accupic 1330 helium pycnometer, Creil, France), was equal to  $1.58 \text{ g cm}^{-3}$ . Fibres architecture is depicted in Fig. 1. The basic unit consists of cellulose polymeric chains aligned and gathered in microfibrils. They are linked to each other by lignin, pectin and hemicellulose. The strength and stiffness of the fibres are provided mostly by hydrogen bonds between the different chemical components. Other characteristics like thermal stability, resistance to UV attack or biodegradation depend on the concentration of each component characterised by its individual properties. Hemicellulose is responsible for the biodegradation, moisture absorption and thermal degradation of the fibre.<sup>13</sup> Lignin and pectin are thermally stable but are responsible for the UV degradation of the fibre.

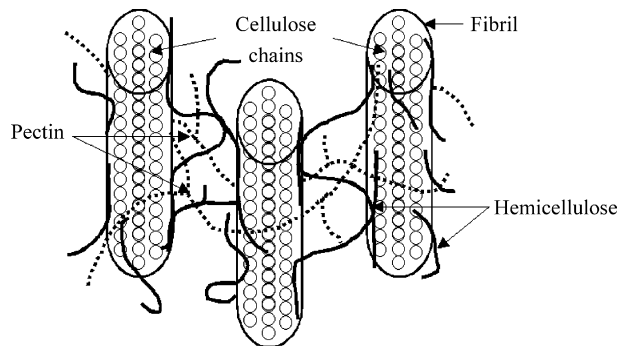


Fig. 1. Hemp fibre architecture.

The quantity of cellulose, hemicellulose, lignin, pectin and fat or waxes contained in hemp was determined after successive extractions.<sup>14</sup> Table 1 lists the chemical composition of hemp fibres. They contain 56.1 wt.% of cellulose, 20.1 wt.% of pectin, 10.9 wt.% of hemicellulose and 6 wt.% of lignin. These values are in accordance with literature data on chemical analysis of natural fibres.<sup>15</sup> Table 2 gives the mass percentage in neutral sugars and acids for each fraction.

A Portland cement (52.5R; CP2 from Lafarge, France) was homogenised, sampled and sifted in order to obtain a granular size below  $40 \mu\text{m}$ . The density was  $3.15 \text{ g cm}^{-3}$ . In order to mimic a solution which forms when cement is mixed with water, we prepared calcium rich and alkaline solution. The hemp fibres were immersed in a lime-saturated solution (calcium concentration:  $22 \times 10^{-3} \text{ mol L}^{-1}$ ).

#### 2.1.2. Fibre surface treatment

In order to modify and possibly improve the adhesion between the fibres and the matrix, the fibres were subjected to different surface treatments. One treatment was with a sodium hydroxide solution and noted FIBNA and a second with a chloride aluminium solution and noted FIBAL. Sodium hydroxide (NaOH) is the most commonly used chemical for bleaching

Table 2  
Molar percentage of each neutral sugar and acid contained in 1 g of hemp

Ose type	Molar percentage ( $\pm 0.1\%$ )
Glucose	69.1
Galacturonic acid	11.6
Xylose	5.5
Rhamnose	4.0
Galactose	3.7
Mannose	2.6
Arabinose	1.9
Glucuronic acid	1.4
Fucose	0.2

and/or cleaning the surface of plant fibres. This treatment was chosen to change both the mechanical properties, like tensile modulus and tensile strength, of the fibres and their surface morphology.<sup>16</sup> In addition this treatment is well known as an effective and cheap one.<sup>17,18</sup> The other treatment with the  $\text{AlCl}_3$  solution was chosen to compare the effect between an alkaline and a slight acid treatment on hemp fibres surface<sup>14</sup> and specifically on their adhesion in a cement matrix.

Concerning the alkaline treatment, fibres were soaked in a 6 wt.% NaOH aqueous solution in a water bath where the temperature was maintained throughout at  $20 \pm 2^\circ\text{C}$  for 48 h. The treated fibres were washed several times with distilled water containing 1 wt.% of acetic acid in order to neutralize the excess of NaOH. Then, they were rinsed in distilled water solution until all the sodium hydroxide was eliminated (neutral pH measured for the fibres washing water).

Fibres were also treated with a 1 wt.%  $\text{AlCl}_3$  solution at room temperature and then rinsed in distilled water solution.

All the fibre, treated and non-treated (FIB), were finally dried in an oven during 48 h at  $60^\circ\text{C}$ .

### 2.1.3. Manufacture of composites

Prior to paste preparation, the fibres were shortening to about 2 cm long and separated in a laboratory mincer (Waring Laboratory, Torrington, USA). The final fibre length ranged between 1 mm and 1 cm. This shortening was necessary to obtain a homogeneous distribution of the fibres in the cement paste. In order to prepare a mix, the pre-cut fibres were introduced in the cement, mixed for 2 min in a blender (Perrier Labotest, type 32, France) and water was finally added. In all cases, the water over cement mass ratio (W/C) was equal to 0.5.

## 2.2. Methods

### 2.2.1. Induced coupled plasma spectroscopy (ICP)

Qualitative and quantitative analysis of elements (calcium, silicium, aluminium, iron) were carried out on solutions that were extracted by centrifugation following the protocol given in Ref. 14. The used equipment was an Iris

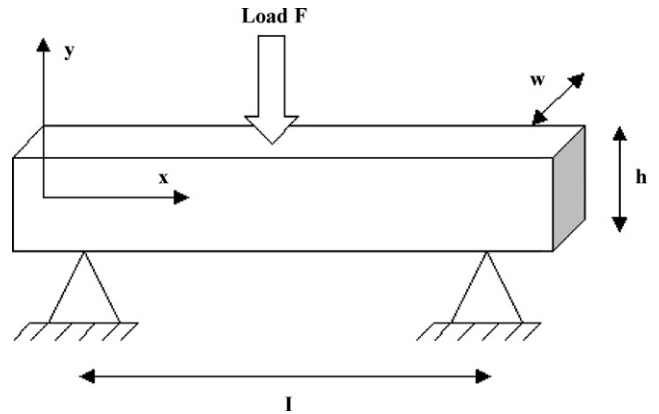


Fig. 2. Scheme of the three point bending test.

Plasma Spectrometer from Thermo Jarrel Ash brand (Waltham, United States).

### 2.2.2. Scanning electron microscopy (SEM)

Scanning electron microscopy (SEM) was carried out with a Cambridge Stereoscan S260 apparatus, equipped with an energy dispersive spectroscopy (EDS) analysis. Characterisation was done on cortical fibres soaked in a lime solution (water over fibres mass ratio: 100). Prior to SEM evaluation, after drying on a blotting paper, fibres were glued directly on a carbon film on a sample holder and samples were coated with gold using a vacuum sputter coater.

SEM experiments were carried out on the fracture surface of the composites, after mechanical testing. Prior to the analysis, the samples were coated with palladium (layer thickness  $\approx 30$  nm) to avoid sample charging under the electron beam.

### 2.2.3. Vicat test

To determine the start and the end of setting time of cement pastes containing or not fibres, a Vicat apparatus was used. The Vicat test<sup>19</sup> was carried out on mixtures of water and cement (W/C=0.5), or mixtures of water with cement and cortical fibres. In this last case, the percentage of hemp was equal to 2 vol.%.

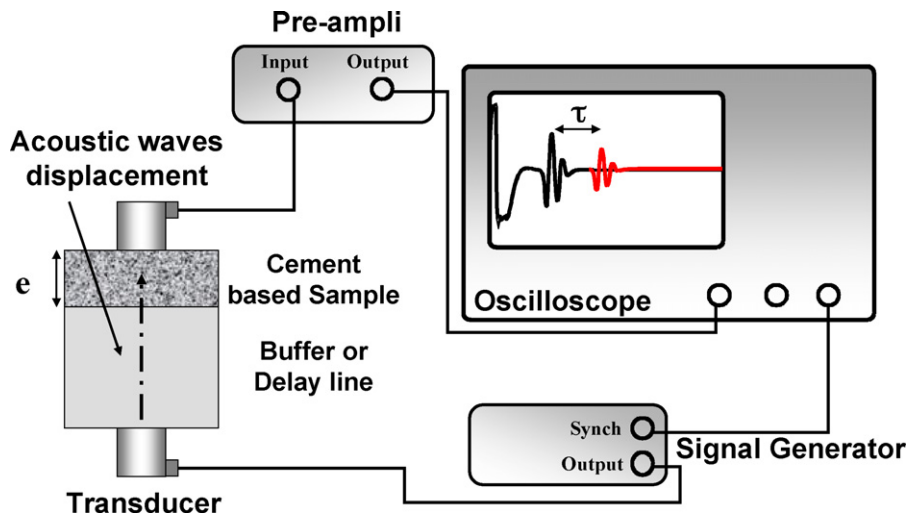


Fig. 3. Experimental setup for ultrasonic measurements.

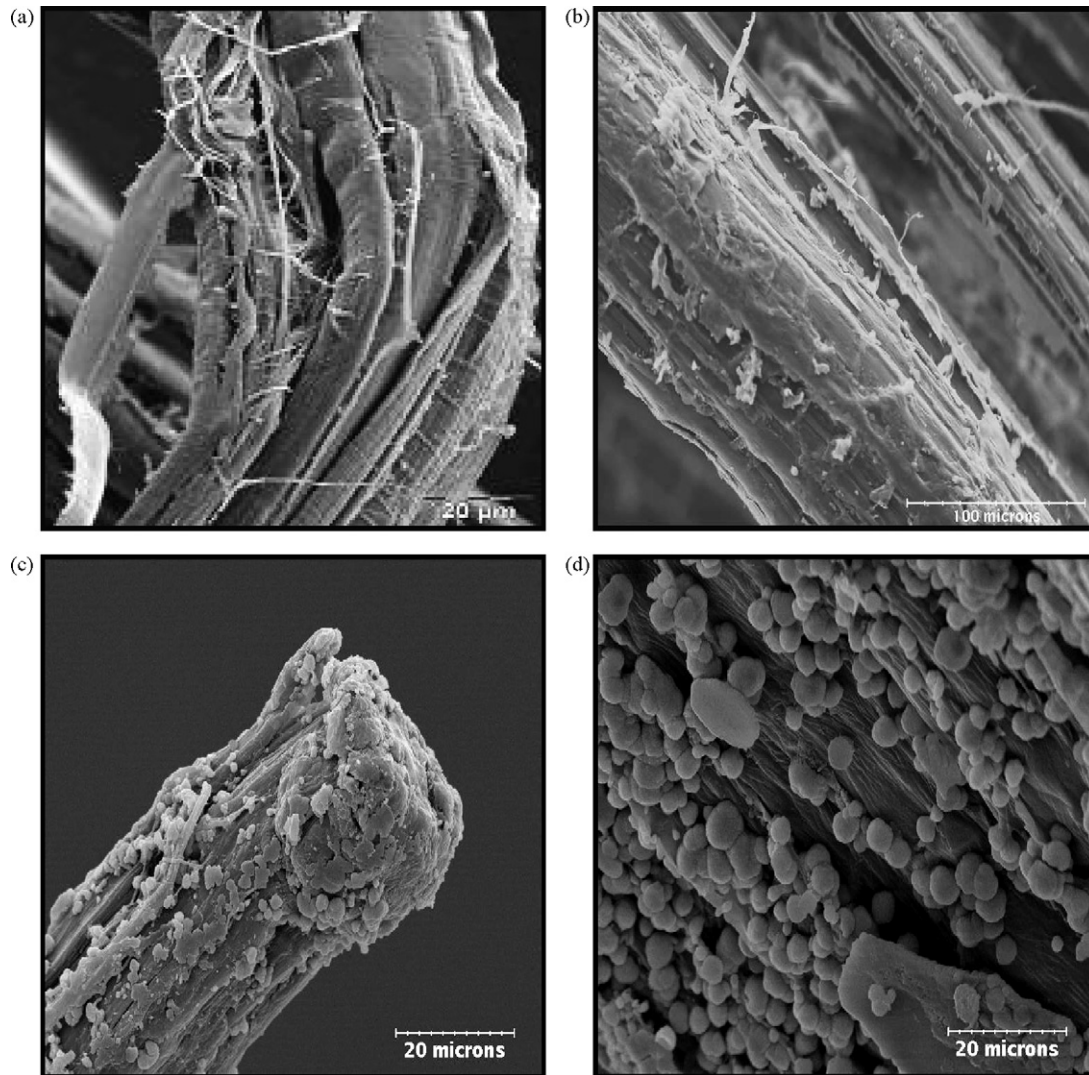


Fig. 4. SEM micrographs of cortical fibres before (a and b) and after immersion in a lime-saturated solution (c and d).

#### 2.2.4. Three point bending test

The three point bending test was carried out using the EZ 20 Lloyd Instrument (AMETEK) testing machine in accordance with AFNOR NF-EN-993-6. Specimen containing between 0 and 20 vol.% of untreated fibres were tested. Prisms with dimensions 40 mm × 40 mm × 160 mm were made from prepared mixtures as described in Section 2.1.3. Samples were covered with a damp polyethylene film in order to avoid water evaporation and then stored in a climatic chamber at  $20 \pm 2^\circ\text{C}$  and  $50 \pm 5\%$  relative humidity. The mechanical test was done on 28 days old specimens. A span of 140 mm and a deflection rate of  $0.1 \text{ mm min}^{-1}$  were used for all tests on this testing machine. At least 12 specimens were tested in a three-point bending configuration for each composite formulation. Value of the load and bending were simultaneously recorded. As we assume that the material is homogeneous, the normal stress  $\sigma_{xx}$  in a rectangular beam (Fig. 2) of length  $l$  between supports is:

$$\sigma_{xx} = \frac{3 Fl}{2 wh^2} \quad (1)$$

in which  $F$  is the applied force and  $w$  and  $h$  are the width and the height of the beam, respectively.

#### 2.2.5. Elastic properties

In order to determine Young's modulus, a non-destructive ultrasonic method was used. These characterisations were done at room temperature. It consists of propagating ultrasonic short pulses across the specimen. These waves are emitted by a transducer (Panametric Sofranel). Transmission pulse echo technique was chosen in order to avoid problems due to the absorbent properties of the composite. This technique enables to measure the transit time related to the ultrasonic velocity. In the present case, the experimental setup is designed to operate in a specific absorbent material (Fig. 3). Different transducers send wideband pulses of longitudinal or transversal ultrasonic waves with a central frequency of 500 kHz, which propagate into a buffer acting as a delay line. The longitudinal or transversal wave velocity has been measured in the transverse direction. The time of flight  $\tau$  (in s) through the samples is related to its thickness  $e$  and the

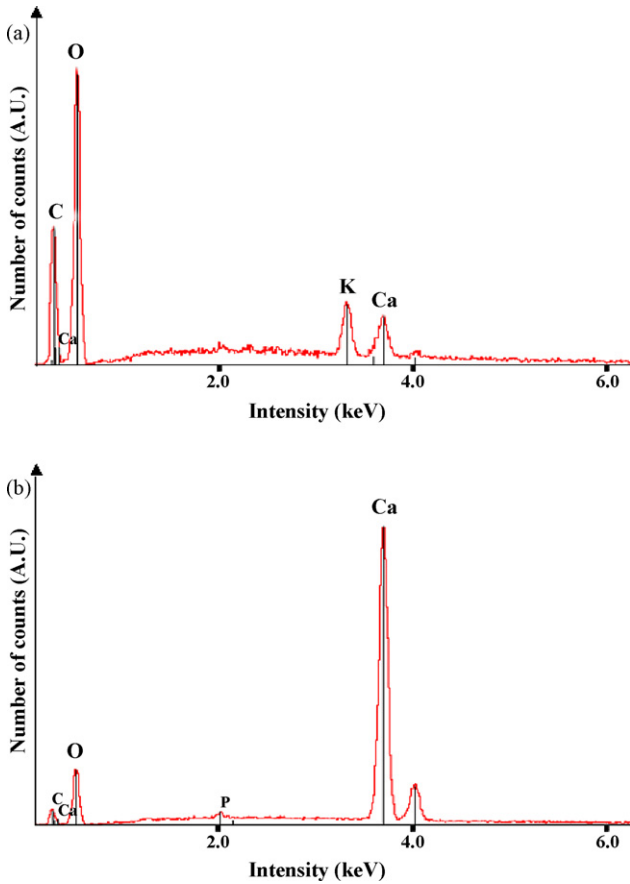


Fig. 5. EDS analysis on a nodule free domain (a) and areas covered with nodules (b).

velocity of the wave, as follows:

$$V = \frac{e}{\tau} \quad (2)$$

The experimental error on  $V$  is of the order of 2%. Measurement of  $\tau$  is obtained according the procedure described elsewhere. Then, Young ( $E$ ) and Shear ( $G$ ) moduli are calculated as follows:

$$E = \rho \frac{3V_L^2 - 4V_T^2}{(V_L^2/V_T^2) - 1} \quad (3)$$

$$G = \rho V_T^2 \quad (4)$$

where  $\rho$  is the sample density,  $V_L$  and  $V_T$  are respectively the longitudinal and transversal wave velocity ( $\text{m s}^{-1}$ ). Finally, the Poisson ratio  $\nu$  is determined using the formula:

$$\nu = \frac{E}{2G} - 1 \quad (5)$$

### 3. Results and discussion

The results on the interactions between the hemp fibres and the lime solutions or the cement matrix are analyzed below. The mechanical behaviour of the hemp–cement composites is discussed in the following section.

Table 3  
Results of the Vicat test

Composition	Component of the mixture	
	Water and cement	Water, cement and 2 vol.% of cortical fibres
Beginning of setting time (Vicat test)	265 min	340 min
End of setting time (Vicat test)	308 min	380 min

#### 3.1. Chemical behaviour of hemp fibres in a cementitious environment

Fig. 4 shows micrographs of cortical fibres before (a and b) and after immersion for 24 h in a lime-saturated solution (c and d). Fig. 4a and b shows packets of aligned microfibrils.<sup>5,10</sup> After immersion in a lime-saturated solution, spherical nodules are sitting on the hemp fibres as it shown in Fig. 4c and d. In order to determine the chemical nature of these nodules, we performed a comparative EDS analysis on areas covered with nodules and a nodule free domain (Fig. 5). Fig. 5b shows that the nodules are calcium rich compared to a nodule free region (Fig. 5a). This suggests that chemical components present in the fibres can trap calcium, which could explain the decrease of calcium ions concentration in the solution as shown in a previous study.<sup>14</sup> Adsorption measurements previously showed that the fibres adsorb a high quantity of  $\text{OH}^-$  ions which does not depend on the  $\text{Ca}(\text{OH})_2$  concentration.<sup>14</sup>  $\text{OH}^-$  trapping should be due to the free carboxylate and alcohol functions found in the chemical structure of the fibre compounds, in particular in the pectin. These functions are ionised in alkaline media and then, surface fibre carries an electrical negative charge that can interact with calcium ions to form  $\text{Ca}(\text{OH})_2$  nodules. Pectin contained in the fibres can also react with calcium ions in an alkaline environment and form a very stable “egg box” structure responsible of the decrease of  $\text{Ca}^{2+}$  concentration in lime-saturated solutions.<sup>14</sup>

Let us examine the case of a mixture with a fix water over cement mass ratio. Samples of Portland cement ( $W/C = 2$ ) were mixed with different fibre contents. After 30 min, the mixtures were centrifugated, the aqueous phase was extracted and the calcium, silicium, aluminium and iron concentration were determined by ICP (Fig. 6). First, it confirms the previous observation that fibres fixed  $\text{Ca}^{2+}$  on their surfaces. The calcium concentration in supernatant decreases from 1300 to 1100 ppm when the fibre quantity increases from 0 to 7 vol.%. A remarkable increase in silicium and to a lesser extend, in aluminium and iron concentrations is recorded for a volumic percentage of fibres greater

Table 4  
Mechanical properties of the cement matrix and its reinforcement

	Young's modulus $E$ (GPa)	Tensile strength (MPa)
Cement matrix	17.3	4.9
Hemp fibres <sup>17,23</sup>	38–58	591–857

Table 5  
Bending test results as function of fibres content

Fibres content (vol.%)	$\sigma_{\max}$ (MPa)	Experimental rigidity (kN/mm)		Decreases of the rigidity after $F^*$
		Before $F^*$	After $F^*$	
0 (cement paste)	4.9	8.0	–	–
7	5.0	5.32	4.78	10.1%
10	5.9	5.29	4.63	11.9%
16	6.8	5.26	4.86	8.2%
20	4.0	4.37	3.41	22.0%

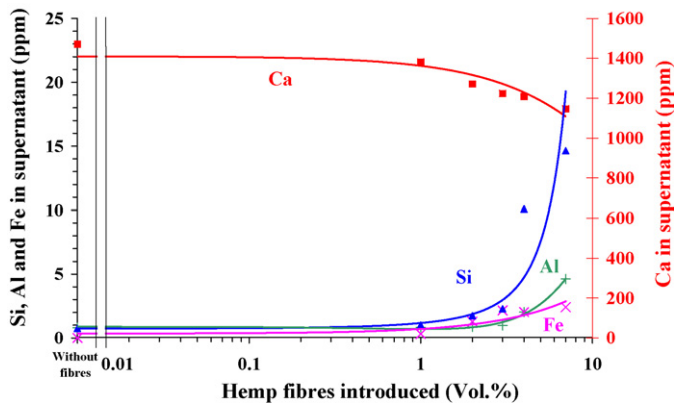


Fig. 6. Variations of the calcium ( $\square$ ), silicium ( $\Delta$ ), aluminium (+) and iron ( $\times$ ) concentrations as function of the quantity of hemp fibres introduced in a diluted cement paste (W/C = 2). Measurements done 30 min after the beginning of mixing.

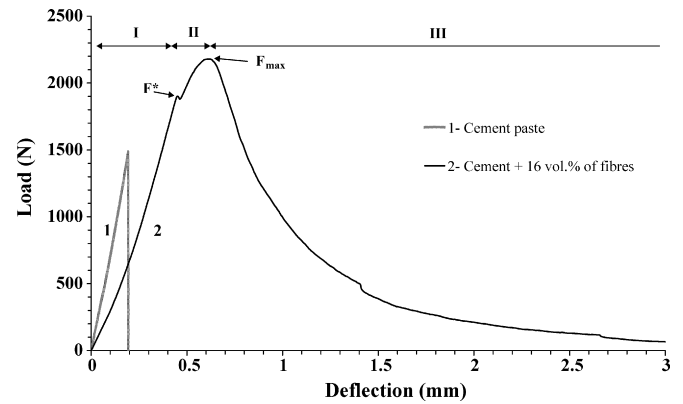


Fig. 7. Example of flexural load–deflection curves for cement paste sample (1) and hemp cement based composite (2).

than 1 vol.%. These results show a change in calcium over silicium ratio. In fact, during the early stages of hydration of a cement paste with W/C of 2.0, this ratio is of the order of 1300.<sup>20,21</sup> However, when 7 vol.% of fibres is introduced, this ratio falls to 60.

### 3.2. Influence on the setting time

Results of the Vicat test (Table 3) show that the introduction of cortical fibres in cement paste delays the beginning of setting time by 45 min. The total duration of setting is similar in the two cases and equal to about 75 min. So, we can observe that a small volume of hemp fibres introduced is sufficient to delay the setting time. Consequently it seems interesting to understand the reasons of this phenomenon to have a better knowledge of the interactions between hemp and cement matrix.

The results discussed in Section 3.1 could explain this delay in setting time. Indeed, we have seen that fibres fix calcium. As we increase the quantity of fibres, the silicium concentration increases in solution or in cement paste (Fig. 6) because it cannot precipitate with calcium to form calcium silicate hydrates (CSH) responsible for setting. Pectin, which can trap calcium, acts as a growth inhibitor for CSH hydrates, which is the major hydration product of Portland cement.<sup>22</sup> So, pectin and consequently fibres by their calcium adsorption will prevent the precipitation of CSH and allow silicium to be retained in solution.

### 3.3. Mechanical properties of the composite

The mechanical properties in a composite depend mostly on the fibre content and orientation, and also on the quality of the load transfer between the matrix and the reinforcement. This fact is closely related to the strength of the interface and consequently to the quality of bonding between the matrix and the fibres. This is particularly true for short fibres reinforced composites due to the multiplication of interfaces. This effect is also magnified by the random orientation of the fibres in the composite.

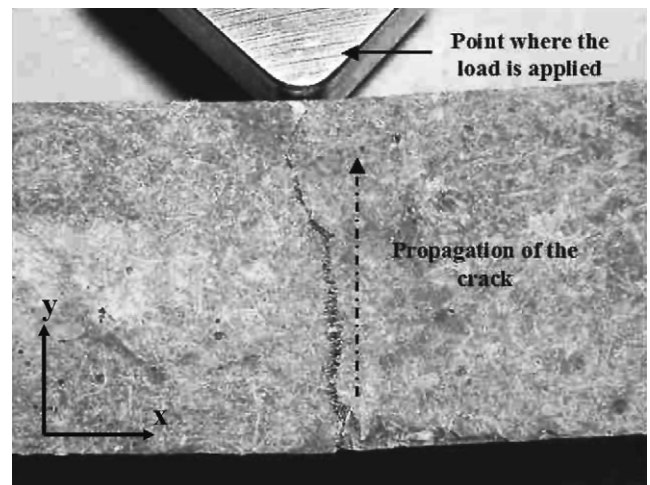


Fig. 8. Propagation of the crack in the composite during the three point bending test.

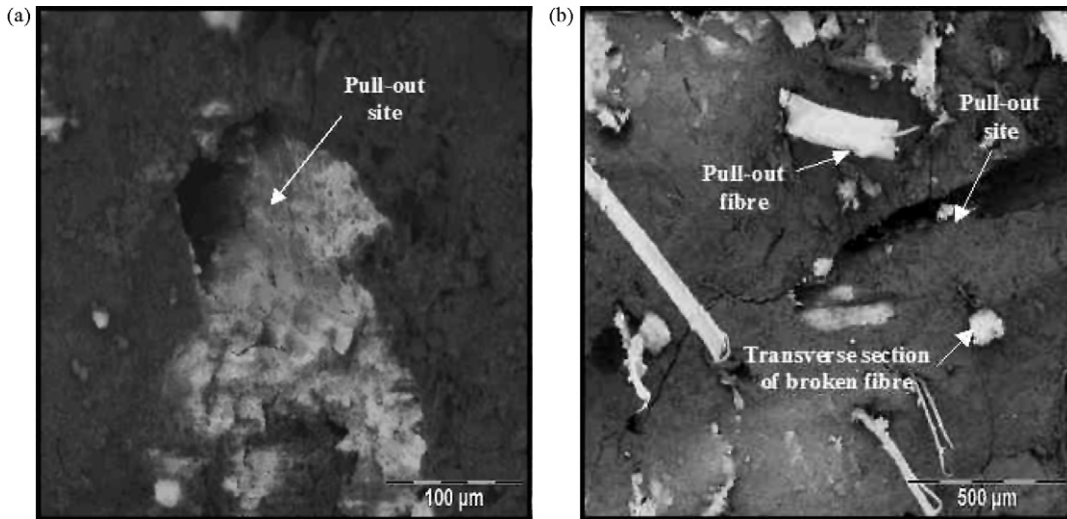


Fig. 9. SEM micrographies of the composite after three point bending test illustrating pull-out site (a) and rupture fibres (b).

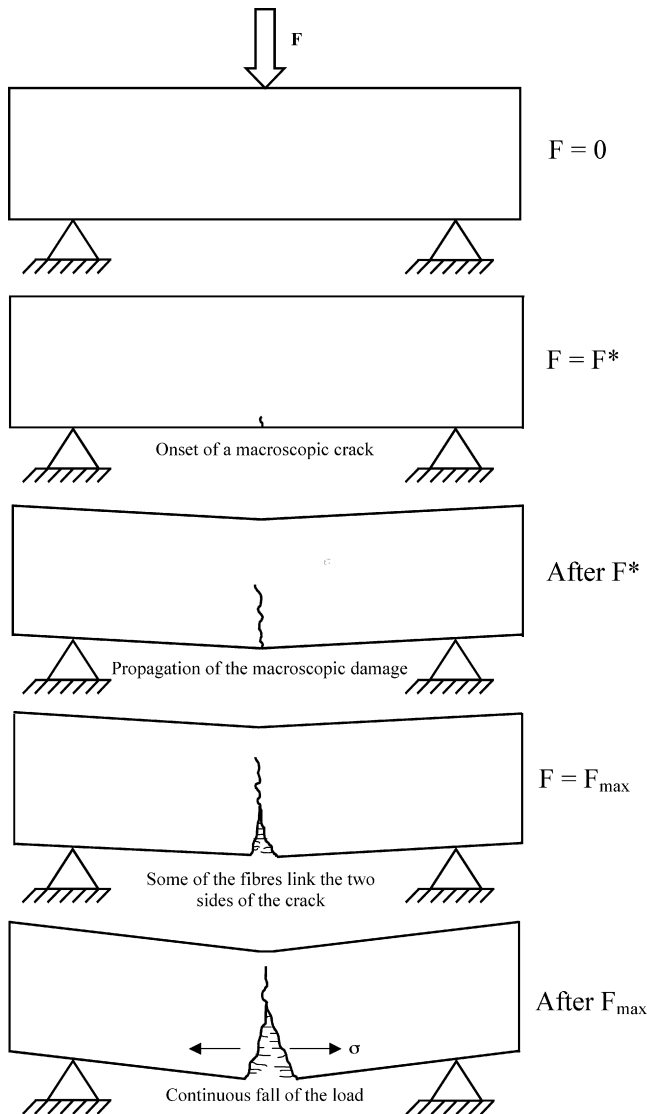


Fig. 10. Chronology of loading and associated mechanical behaviour of the composite.

### 3.3.1. Mechanical behaviour analysis

Table 4 gives the mechanical properties of the cement matrix and the reinforcement, separately. We can see that hemp fibres have a higher tensile strength and Young’s modulus than the matrix. Concerning the flexural behaviour of the different materials, Fig. 7 shows an example of flexural load–deflection curves for a cement paste sample (1) and a hemp cement based composite (2). Two different types of curves are observed. The first one concerning cement paste sample is characterised by a linear brittle behaviour. The second one exhibits a typical composite behaviour. The evolution of the load versus the central deflection of the sample can be divided into three parts separated by two characteristic force values. The critical load  $F^*$ , which can be considered probably as the initial pull-out debonding force, and the peak load  $F_{max}$ , which can be interpreted as the highest failure force (closely related to the pull-out failure force).

Region I [ $0-F^*$ ] presents a linear evolution of the load versus deflection as quoted for the cement sample. In this step, it seems that the matrix is supporting the main part of the applied load. Region II begins at  $F^*$  which corresponds to the load where a notable change of the stiffness is observed (Table 5). This specific point marks the occurrence of the first macroscopic damage in the material. Indeed, since this critical load point, the onset of a macroscopic crack (Fig. 8) can be easily observed on the sample. In this picture, we can see that some of the fibres are debonded on both side of the crack. We can also observe that some of the fibres link the two sides of the crack. Initially, the fibres in the composite are randomly oriented. During the bending test, their direction becomes more and more perpendicular

Table 6  
Influence of the fibres treatment

Composites	$\sigma_{max}$ (MPa)	$E$ (GPa)	$G$ (GPa)	Nu
Cement paste	4.9	17.2	6.9	0.254
FIB	6.8	12.9	5.3	0.215
FIBNA	9.5	13.1	5.3	0.230
FIBAL	7.3	12.7	5.1	0.238

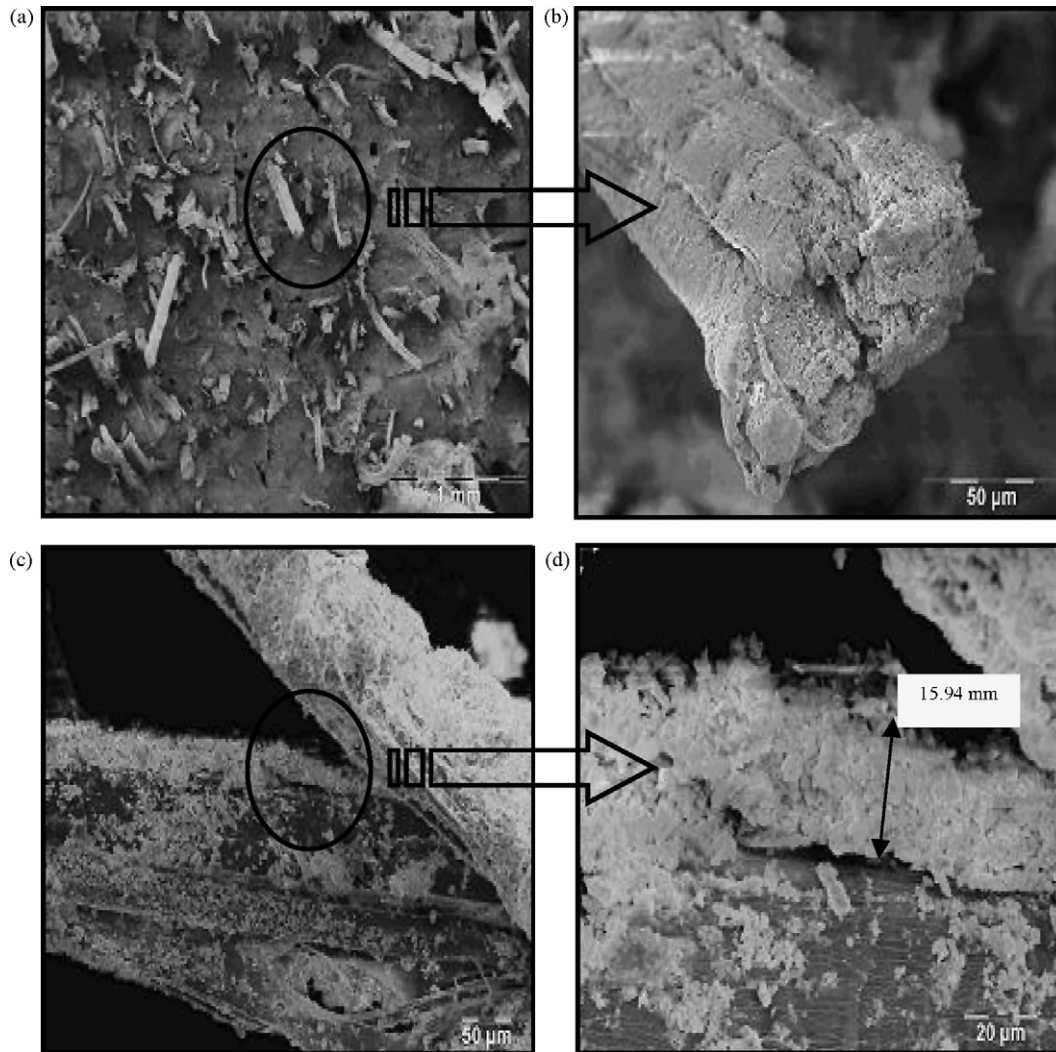


Fig. 11. SEM micrographies of sample fracture surface of hemp–cement composite (16 vol.%) after three point bending test.

to the direction of the load as it increases. This process leads to a pull-out phenomenon (Fig. 9) which disturbs the load transfer process. Beyond  $F^*$  and up to  $F_{\max}$ , a significant fall of the experimental stiffness is recorded as well as the force continues to increase. The experimental stiffness is calculated from the linear part of the slope of the load–deflection curve taken before and after  $F^*$ . In a fibre pull-out processing, the applied load is transferred and distributed along the fibre/matrix interface and causes interfacial failure. This continuous controlled debonding process of the fibres at the cement matrix interface is associated to a controlled phase of the crack propagation. After the peak load  $F_{\max}$  (region III), the mechanical behaviour is totally different than the one observed for the cement sample. This part is very interesting because it reveals the change in behaviour mostly due to the presence of fibres in the composite. Indeed, no sudden failure is observed but a continuous fall of the load is recorded. This behaviour underlines the major role of the debonding process on the ruin of the material. Fig. 10 summarises the different steps presented above. Fig. 11 shows micrographs of fracture surfaces. We can observe that the fibres are entirely covered with nodules identified as calcium rich by

EDS analysis. This calcium “coating” (Fig. 10b), can exhibit a large thickness ( $\approx 16 \mu\text{m}$ ). This coating sometimes irregularly distributed at the fibre/matrix interface can explain the behaviour of the material.

### 3.3.2. Effect of fibre content

The results of the bending tests for composites are presented in Table 5 as a function of fibres content, which varied between 0 and 20 vol.%. Firstly, if we make a comparison between the composites, we can observe that the maximal flexural strength is reached for an optimal fibre fraction of 16 vol.%. This property has been already observed in others studies.<sup>24</sup> Until 16 vol.%, a progressive increase of the material strength can be recorded, due to a high quantity of fibre–matrix interface. Beyond this fibre fraction, the flexural strength of the composite decreases due to a non-homogeneous mix and, consequently, a poor adhesion between the fibres and the matrix. Lastly, if we compare the mechanical properties between the composite with the optimal fibre content and the cement alone, the gain of flexural strength  $\sigma_{\max}$  is about 40% for the first one. However, in the same time, a notable fall of the experimental rigidity is noted (around 35%).



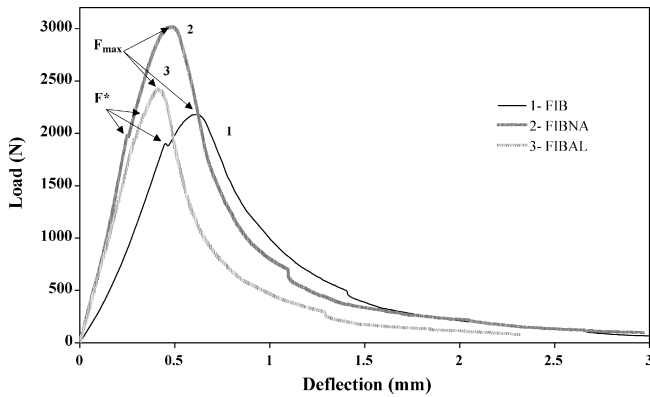


Fig. 12. Load–deflection curves for FIB, FIBNA and FIBAL from flexural test.

To sum up, the fibres network in composites permits an increase of the flexural strength associated to a rise of the displacement to rupture.

### 3.3.3. Effect of fibre surface treatment

Composites studied in this part contain the optimal fibre fraction (16 vol.%). Table 6 shows the influence of the fibres treatment on the mechanical properties of the composite. It can be observed that a notable effect is recorded on the flexural properties when untreated hemp fibres are replaced by NaOH or  $\text{AlCl}_3$  treated fibres. Concerning flexural strength, an improvement of at least 39% for FIBNA and 7% for FIBAL is quoted compared to the FIB composite. Compared with the cement paste alone the gain in flexural strength is 94% for FIBNA and 49% for FIBAL. Fig. 12, corresponding to load–deflection responses for FIB, FIBNA and FIBAL, illustrates this increase of flexural strength. These curves exhibit the same mechanical behaviour than for the untreated fibres composites. However, it is found that treated fibre specimens have both higher critical and peak loads. This means that the interfacial adhesion strength gets stronger after a chemical treatment.

The treatment with the aqueous solution of NaOH removes some hemicelluloses, waxes and impurities from the fibre surface. The surface is chemically more homogeneous. It has also been observed that treatment with NaOH tends to roughen the fibre surface.<sup>14,24,25</sup> The consequence is a global improvement of the load transfer process at the interface. These changes in morphology and in chemical composition of the fibres participate to an upgrading of the contact between the fibres and the matrix and to the enhancement of the mechanical properties, especially the flexural strength (Table 6). Mwaikambo et al. have also shown that an optimal tensile strength of the fibre is obtained for a NaOH concentration of 6 wt.% resulting in a cleaning of the hemp fibre bundle surface.<sup>26,27</sup> Consequently, the gain of the flexural strength in our composite can be attributed not only to the improvement in adhesion at the interface but also to the improvement of the fibre tensile strength. Concerning  $\text{AlCl}_3$  treated fibres, the effect of the treatment on the flexural strength of the composite is less notable. Indeed, it permits only the removal of impurities or waxy substances on their surface and has little effect on fibres morphology.<sup>14</sup> This slight surface cleaning compared to NaOH treatment shows that the

adhesion between the cement matrix and the fibres is a key parameter.

Table 6 also presents the values of the elastic moduli and Poisson's ratios of the composites measured at 28 days. The composite samples have lost some rigidity compared with the cement sample. Young's modulus decreases strongly from  $17.2 \pm 0.2$  GPa for cement pastes to  $12.9 \pm 0.5$  GPa for FIB composites (Table 6). Therefore, none of the improvement of the fibre–matrix interface (FIBNA or FIBAL) had a significant effect on the value of Young's modulus (Table 6). Within the experimental errors it can be said that Young modulus of FIB, FIBNA ( $13.1 \pm 0.3$  GPa) and FIBAL ( $12.7 \pm 0.1$  GPa) composites are fairly equal. Consequently, if the treatments have no beneficial effect on Young's modulus, it increases considerably the flexural strength of the composite, especially for FIBNA.

## 4. Conclusion

Several interesting conclusions can be extracted from this study. Concerning the fibre–matrix chemical interactions, hemp fibres seem to trap calcium on their surface. Pectins can fix calcium through a complex structure called “eggs box”. This calcium fixation could be responsible for the delay in setting time, by the fact that pectins act as a growth inhibitor for calcium silicate hydrates.

Concerning the composite mechanical behaviour, it was observed a strong increase of the flexural strength for an optimal fibre content. It can be seen that for a composite containing 16 vol.% of fibres, the flexural strength is maximal and about 40% higher than that of the cement paste. It is equally observed a decrease of the composite Young's modulus compared to the cement paste. Indeed, treatments applied on hemp fibres in this study improve only the flexural strength. An alkaline treatment improves this strength of about 94% compare to the cement paste. Alkali treatment affects not only the fibre strength, but also the fibre–matrix adhesion in a positive way. Such composites could be consequently interesting in building applications.

## References

- Bledzki, A. K. and Gassan, J., Composites reinforced with cellulose based fibres. *Prog. Polym. Sci.*, 1999, **24**, 221–274.
- Gassan, J., A study of fibre and interface parameters affecting the fatigue behavior of natural fibre composites. *Composites Part A*, 2002, **33**(3), 369–374.
- Mishra, S., Tripathy, S. S., Misra, M., Mohanty, A. K. and Nayak, S. K., Novel eco-friendly biocomposites; biofiber reinforced biodegradable polyester amide composites: fabrication and properties evaluation. *J. Reinf. Plast. Comp.*, 2002, **21**(1), 55–70.
- O'Donnell, A., Dweib, M. A. and Wool, R. P., Natural fibre composites with plant oil-based resin. *Compos. Sci. Technol.*, 2004, **64**, 1135–1145.
- Hepworth, D. G., Holson, R. N., Bruce, D. M. and Farrent, J. W., The use of unretted hemp fibre in composite manufacture. *Composites Part A*, 2000, **31**, 1279–1283.
- Pearce, E. M., Fibre chemistry. *Handbook of Fibre Science and Technology, Vol IV*. Menachem Lewin Eli M. Pearce, New York, 1985, pp. 737–746.
- Gassan, J. and Bledzki, A. K., The influence of fibre-surface treatment on the mechanical properties of jute–polypropylene composites. *Composites Part A*, 1997, **28**, 1001–1005.
- Scrivener, K. and Van Damme, H., Construction materials: from innovation to conservation. *MRS Bull.*, 2004, 308–312.

9. Zhu, W. H., Tobias, B. C., Coutts, R. S. P. and Langfors, G., Air-cured banana-fibre-reinforced cement composites. *Cement Concrete Compos.*, 1994, **16**(1), 3–8.
10. Tolêdo Filho Romildo, D., Ghavami, K., England, G. L. and Scrivener, K., Development of vegetable fibre-mortar composites of improved durability. *Cement Concrete Compos.*, 2003, **25**, 185–196.
11. Li, Z., Wang, X. and Wang, L., Properties of hemp fibre reinforced concrete composites. *Composites Part A*, 2005, 1–9.
12. Singh, N. B., Singh, V. D. and Rai, S., Hydration of bagasse ash blended portland cement. *Cement Concrete Res.*, 2000, **30**(2), 1485–1488.
13. Sahed, D. N. and Jog, J. P., Natural fibre polymer composites: a review. *Adv. Polym. Technol.*, 1999, **18**(4), 351–363.
14. Sedan, D., Pagnoux, C., Chotard, T., Smith, A., Lejolly, D., Gloaguen, V. and Krausz, P., *Journal of Material Science*, 2007, in press.
15. Garcia-Jaldon, C., Dupeyre, D. and Vignon, M. R., Fibres from semi retted hemp bundles by steam explosion treatment. *Biomass Bioenergy*, 1998, **14**, 251–260.
16. Sharifa, H. A. and Ansell, M. P., The effect of alkalization and fibre alignment on the mechanical and thermal properties of kenaf and hemp bast fibre composites. *Compos. Sci. Technol.*, 2004, **64**, 1219–1238.
17. Pickering, K. L., Beckermann, G. W., Alam, S. N. and Foreman, N. J., Optimising industrial hemp fibre for composites. *Composites Part A*, 2007, **38**, 461–468.
18. Van de Weyenberg, I., Chi Truong, T., Vangrimde, B. and Verpoest, I., Improving the properties of UD flax fibre reinforced composites by applying an alkaline fibre treatment. *Composites Part A*, 2005, **37**(9), 1366–1376.
19. Dupain, R., Lanchon, R. and Saint-Arroman, J.-C., *Granulats, sols, ciments et bétons*. A. Clapiez, 1995, pp. 99–103.
20. Thomas, N. L. and Double, D. D., *Cement Concrete Res.*, 1981, **11**, 675.
21. Thomas, N. L. and Birchall, J. D., The retarding action of sugars on cement hydration. *Cement Concrete Res.*, 1983, **13**, 830–842.
22. Double, D. D., Thomas, N. L. and Jameson, D. A., In *Proceedings of the 7th International Congress of Cement Chemistry, Vol 2*, 1980, p. II-256.
23. Mwaikambo, L. Y. and Ansell, M. P., Hemp fibre reinforced cashew nut shell liquid composites. *Compos. Sci. Technol.*, 2003, **63**, 1297–1305.
24. Nam-Jeong, L. and Jyongsik, J., The effect of fibre-content gradient on the mechanical properties of glass-fibre-mat/polypropylene composites. *Compos. Sci. Technol.*, 2000, **60**, 209–217.
25. Valadez-Gonzales, A., Cervantes-Uc, J. M., Olayo, R. and Herrera-Franco, P. J., Effect of fiber surface treatment on the fiber–matrix bond strength of natural fiber reinforced composites. *Composites Part B*, 1999, **30**, 309–320.
26. Mwaikambo, L. Y. and Ansell, M., Chemical modification of hemp, sisal, jute, and kapok fibers by alkalisation. *J. Appl. Polym. Sci.*, 2002, **84**, 2222–2234.
27. Gassan, J. and Bledzki, A. K., Possibilities for improving the mechanical properties of jute/epoxy composites by alkali treatment of fibres. *Composites Sci. Technol.*, 1999, **59**, 1303–1309.